A01-16862

AIAA 2001-1077

SOOT SURFACE GROWTH IN LAMINAR HYDROCARBON/AIR DIFFUSION FLAMES AT ATMOSPHERIC PRESSURE

A.M. El-Leathy, F. Xu and G.M. Faeth
Department of Aerospace engineering
The University of Michigan
Ann Arbor, Michigan 48109-2140

39th AIAA Aerospace Sciences Meeting & Exhibit
8-11 January 2001 / Reno, NV

2001-1077

SOOT SURFACE GROWTH IN LAMINAR HYDROCARBON/AIR DIFFUSION FLAMES AT ATMOSPHERIC PRESSURE

by

A.M. El-Leathy,* F. Xu† and G.M. Faeth‡

The University of Michigan, Ann Arbor, Michigan 48109-2140

Abstract

The soot surface growth and flame structure properties of round laminar coflowing jet diffusion flames were studied experimentally. Test conditions involved ethylene-, propylene- and propane-fueled diffusion flames burning in coflowing air at atmospheric pressure. Measurements were limited to the axes of the flames and included soot concentrations, soot temperatures, soot structure, major gas species concentrations, radical (H,OH,O) species concentrations, and gas velocities. The results show that fuel decomposition yields significant acetylene concentrations at fuel-rich conditions, that significant soot formation begins when significant H-radical concentrations are present, and soot formation ends when acetylene concentrations become small. Hydrogen, OH and O radicals are present throughout the soot formation region so that soot formation and oxidation proceed at the same time. Strong rates of soot growth compared to rates of soot nucleation early in the soot formation process, combined with increased rates of soot nucleation and oxidation as soot formation proceeds, causes primary soot particle diameters to reach a maximum relatively early in the soot formation process. Present measurements in diffusion flames exhibit encouraging agreement with existing Hydrogen-Abstraction/Carbon-Addition (HACA) growth mechanisms, with earlier soot growth measurements in acetylene-fueled diffusion flames, and with earlier soot growth measurements in premixed flames fueled with a variety of hydrocarbons.

Nomenclature

d	= fuel port exit diameter (m)
d_p	= mean primary soot particle diameter (m)
f_S	= soot volume fraction (-)
Fr	= burner exit Froude number (-), $u_o^2/(gd)$
g	= acceleration of gravity (ms^{-2})
$[i]$	= molar concentration of species i ($kgmol\ m^{-3}$)
n_p	= number of primary particles per unit volume (m^{-3})
R_i	= terms in the HACA soot surface growth rate formulas ($kg\ m^{-2}s^{-1}$)
Re	= burner exit Reynolds number (-), $u_o d/\rho_o$
S	= soot surface area per unit volume (m^{-1})
t	= time (s)
T	= temperature (K)
u	= streamwise velocity (ms^{-1})
w_g	= soot growth rate ($kg\ m^{-2}s^{-1}$)
w_n	= soot nucleation rate ($mol\ m^{-3}s^{-1}$)
z	= streamwise distance (m)
α_i	= empirical (steric) factors in the HACA soot surface growth formulas
ν	= kinematic viscosity (m^2s^{-1})
ρ	= gas density ($kg\ m^{-3}$)
ρ_S	= soot density ($kg\ m^{-3}$)
ϕ	= fuel-equivalence ratio (-)

Subscripts

CH	= HACA soot growth mechanism of Colket and Hall[11]
FW	= HACA soot growth mechanisms of Frenklach and coworkers[8-11]
o	= burner exit condition

*Research Scholar, Department of Aerospace Engineering.

†Research Associate, Department of Aerospace Engineering.

‡A.B. Modine Professor, Department of Aerospace Engineering; Fellow, AIAA.

Introduction

The presence of soot is a common feature of nonpremixed (diffusion) flames fueled with hydrocarbons, affecting their structure and reaction mechanisms. As a result, soot processes affect capabilities for computational combustion due to the complexities of soot chemistry, public health due to emissions of particulate soot, fire safety due to increased fire growth rates caused by soot radiation, and combustor durability due to undesirable heat loads caused by continuum radiation from soot. Motivated by these observations, the present investigation sought to extend past work on soot surface growth in laminar premixed and diffusion flames in this laboratory, see Refs. 1-7, seeking to evaluate theoretical predictions of soot surface growth rates in hydrocarbon-fueled coflowing jet diffusion flames in air at atmospheric pressure.

Sunderland and coworkers[1-3] experimentally studied soot surface growth in laminar hydrocarbon/air diffusion flames by making direct measurements of soot residence times, soot concentrations, soot structure, gas temperatures, and the concentrations of stable gas species. It was found that soot surface growth only occurred when acetylene was present and that growth rates were roughly first-order with respect to acetylene concentrations. Existing detailed soot surface growth models,[8-11] however, could not be evaluated using these results because radical species concentrations important for these mechanisms were not measured.

Xu et al.[4-6] extended Sunderland and coworkers[1-3] by considering soot surface growth in premixed flames. Experimental methods were similar to Sunderland and coworkers[1-3] except that concentrations of radical species (H, OH and O) were determined both computationally and experimentally. It was found that concentrations of H closely approximated equilibrium requirements in the relatively slowly evolving soot growth regions of premixed flames. The new measurements were then used to evaluate the Hydrogen-Abstraction/Carbon-Addition (HACA) soot growth mechanisms of Frenklach and coworkers[8-10] and Colket and Hall.[11] The results showed that the HACA soot growth mechanisms yielded excellent correlations of the measurements of soot surface growth rates for quite reasonable values of the steric factors that appear in the theories.

Xu and Faeth[7] continued study of soot surface growth by considering diffusion flame environments that are more relevant to practical soot formation processes in flames. These experiments involved acetylene/air laminar coflowing jet diffusion flames using the full suite of measurements developed during the earlier studies of premixed flames, e.g., Refs. 4-6. These results showed that H concentrations ranged from near-equilibrium conditions to super-equilibrium ratios of 20-30 in the soot surface growth region of the diffusion flames, that soot surface growth rates in premixed flames and diffusion flames satisfy similar reaction rate expressions, and that soot surface growth rates in these diffusion flames were well represented by the HACA mechanisms of Refs. 8-11, with steric factors essentially unchanged from observations in premixed flames, see Ref. 7.

Naturally, there have been many other studies of the structure and soot processes of laminar hydrocarbon-fueled diffusion flames, seeking detailed models of these properties, see Balthesar et al.[12], Bai et al. [13] and references cited therein. Early measurements of flame structure and soot processes in laminar diffusion flames include Mitchell et al.,[14] Santoro and coworkers,[15-19] Saito et al.,[20] Garo et al.[21,22] and many other studies reviewed by Haynes and Wagner,[23] Howard[24] and Glassman.[25] More recent work along these lines due to Hardequert et al.[26] and McEnally and Pfefferle[27-28] involve rather sophisticated probe and nonintrusive measurements within complex soot-containing laminar diffusion flame environments. None of these studies, however, involved the complex suite of measurements mentioned earlier, and used by Xu and coworkers[4-7] within laminar premixed and diffusion flames, that is needed to evaluate theories of soot growth along the lines of Refs. 8-11.

Based on this status, the present investigation sought to improve understanding of the structure and soot formation properties of laminar diffusion flames, by considering coflowing jet diffusion flames burning in air at atmospheric pressure but using hydrocarbons other than acetylene in order to explore potential modifications of the soot surface growth mechanism when the fuel was no longer a species directly involved with the HACA soot surface growth mechanism, which is the case for acetylene. The specific objectives of the study were as follows: (1) to complete measurements of soot properties (soot volume fractions and primary particle diameters) and flame structure (temperatures, stable and radical species concentrations and velocities) within the soot formation region of the test flames, and (2) to exploit the new measurements to correlate and evaluate the HACA soot surface growth mechanisms of Frenklach and coworkers[8-10] and Colket and Hall[11] for

the present hydrocarbon-fueled diffusion flames and to compare these results with earlier findings for premixed flames[4,5] and acetylene-fueled diffusion flames.[7] The experiments were limited to measurements along the axes of buoyant laminar coflowing jet diffusion flames at atmospheric pressure.

Experimental Methods

Test Apparatus

Experimental methods were very similar to Xu and Faeth[7] and will be described only briefly. The same burner arrangement was used to observe soot processes in laminar diffusion flames and to calibrate the H concentration measurements using a laminar premixed flame. The burner had a 34.8 mm diameter inner port both for the fuel stream flow of the diffusion flames or the methane-oxygen-nitrogen reactant mixture flow for the premixed flame. A 60 mm diameter coannular outer port was used both for the air coflow of the diffusion flames or the nitrogen coflow of the premixed calibration flame. The air coflow of the diffusion flames served to eliminate natural convection instabilities whereas the nitrogen coflow of the premixed flame served to eliminate the annular diffusion flame for this fuel-rich flame in order to improve the accuracy of the H concentration calibration.

Burner gas flow rates were measured with rotameters. Mixtures were allowed to mix within feed lines that were at least 1000 diameters long to ensure that they were uniform. The flames burned in room air with room disturbances controlled by surrounding them with several layers of screens and a plastic enclosure. The burner could be moved horizontally and vertically with linear positioners in order to accommodate rigidly-mounted optical instrumentation.

Instrumentation

Present measurements were similar to Xu and Faeth[7] and will be described only briefly. The following properties were measured along the axes of the flames: soot volume fractions, flame temperatures, concentrations of major stable gas species, soot structure, gas velocities and concentrations of some radical species (H, OH and O).

Soot volume fractions were measured by deconvoluting laser extinction measurements at 632.8 nm for chord-like paths through the flames. Data was reduced using the refractive indices of Dalzell and Sarofim,[29] similar to past work;[1-7] these values have recently been confirmed by Krishnan et al.[30] The experimental uncertainties (95% confidence) of soot volume fractions are estimated to be smaller than 10% for soot volume fractions greater than 0.02 ppm, increasing proportional to the soot volume fraction for smaller values.

Soot and gas temperatures are essentially the same;[7] thus soot (gas) temperatures were measured by deconvoluting spectral radiation intensities for chord-like paths through the flames and computing temperatures at several wavelength pairs (550/700, 550/750, 550/830, 600/700, 600/750, 600/830 and 650/750 nm). Temperature differences between the average and any of the line pairs were less than 50-100 K and experimental uncertainties (95% confidence) of these measurements were less than 50 K.

Concentrations of major gas species (N_2, H_2O, H_2, O_2, CO, CO_2, CH_4, C_2H_2, C_2H_4, C_2H_6, C_3H_6, C_3H_8 and neon, the last being a tracer gas used to estimate effects of radial diffusion of lithium-containing species that were used to find H concentrations) were measured by sampling and analysis by gas chromatography. Experimental uncertainties (95% confidence) of these measurements are mainly due to calibration uncertainties and are estimated to be less than 5% for all species concentrations reported here.

Soot structure measurements were limited to primary soot particle diameters carried out by thermophoretic sampling and analysis by Transmission Electron Microscopy (TEM), following Dobbins and Megaridis[31] similar to earlier work in this laboratory.[32] Primary particle diameters were nearly monodisperse at given positions in each flame (standard deviations were less than 10%) and the experimental uncertainties (95% confidence) of soot primary particle diameter measurements are estimated to be less than 10%.

Streamwise gas velocities were measured using laser velocimetry with experimental uncertainties (95% confidence) less than 5%.

Measurements of H concentrations were carried out by deconvoluted absorption following the Li/LiOH atomic absorption technique of Neoh and coworkers.[33,34] Correction for the radial diffusion of LiOH seed was found from measurements of the concentrations of neon seed, assuming that the diffusivities of LiOH and neon were similar. The H concentration measurements were calibrated using a premixed flame as discussed by Xu and Faeth[6] and

similar to Neoh and coworkers.[33,34] Measurements with different seeding levels showed that effects of LiOH seed on flame properties were negligible, similar to past work.[6,7] Experimental uncertainties (95% confidence) of the H concentration measurements are estimated to be smaller than 30%.

Test Conditions

The properties of the laminar premixed flame used to calibrate the H concentration measurements are reported by Xu and Faeth.[6] The present test flames involved ethylene, propylene-nitrogen and propane fuel streams burning in air as summarized in Table 1. Nitrogen dilution was used for the propylene flame in order to keep maximum soot volume fractions smaller than 2 ppm so that problems of large soot concentrations on the measurements could be avoided. Luminous flame lengths were 85-100 mm whereas stoichiometric flame lengths (the vertical height of the position where the local fuel equivalence ratio at the axis is stoichiometric) were 74 to 81 mm. Reynolds and Froude numbers were 23-92 and 0.00003-0.0009, respectively. Characteristic residence times were taken to be the times for the flow to convect from the point where measurable quantities of soot were first observed to the flame sheet. Finally, adiabatic flame temperatures at the stoichiometric mixture ratio were computed using the algorithm of McBride et al.[35]

Table 1 Summary of the Laminar Hydrocarbon/Air Diffusion Flames[a]

Fuel	Ethylene	Propylene	Propane
Burner flow (% fuel by vol.)	100.0	18.8	100.0
Fuel flow rate (cc/s)	5.52	3.12	3.20
Nitrogen flow rate (cc/s)	---	13.50	---
Air coflow rate (cc/s)	292	222	222
Burner exit velocity (mm/s)	5.8	17.4	3.4
Air coflow velocity (mm/s)	171	130	130
Luminous flame length (mm)	100	100	100
Stoichiometric flame length (mm)	81	74	79
Re(-)[b]	23	92	25
Fr $\times 10^5$ (-)[b]	9.9	89.0	3.3
Characteristic residence time (ms)[c]	66	61	64
Stoichiometric flame temperature (K)[d]	2366	2147	2263

[a]Laminar round jet diffusion flames with a 34.8 mm inside diameter fuel port, flowing fuel-N_2 mixtures and a 60 mm inside diameter outer port flowing air. Ambient temperature of 294 ± 2K and pressure of 98 ± 1 kPa. Gas purities: nitrogen, 99.9%, ethylene, 99.5%, propylene, 99.5%, propane, 99.5%, oxygen, 99.6%, laboratory air coflow with 240 K dewpoint.
[b]Nominal value based on mean burner exit velocity.
[c]Time to convect from first appearance of soot to stoichiometric mixture ratio, $\phi = 1$.
[d]Adiabatic flame temperature for stoichiometric premixed combustion of the burner fuel flow mixture in air at atmospheric pressure.

Results and Discussion

Soot Structure

Present soot particles were similar to soot observed during past studies of soot processes in laminar diffusion and premixed flames, see Refs. 1-7 and references cited therein for photographs of soot particles of various types of flames. The soot particles consisted of roughly spherical primary soot particles that have nearly constant diameters at a particular location, collected into open structured aggregates of various sizes. The maximum numbers of primary soot particles per aggregate progressively increased with increasing distance from the burner exit. Finally, the aggregates exhibited widely varying numbers of primary soot particles per aggregate far from the burner exit, after aggregation had proceeded for a time.

Flame Structure

Measurements of gas (soot) temperatures, streamwise gas velocities, soot primary particle diameters, soot volume fractions, the concentrations of major gas species and the concentrations of radical (H, OH, O) species are plotted as a function of height above the burner exit along the axes of the ethylene, propylene, and propane-fueled flames in Figs. 1-3, respectively. Corresponding residence times, found by integrating the streamwise velocity measurements, are indicated at the top of the plots. The residence times were mainly used to find soot growth rates and are relative to the first position where detectable soot volume fractions were observed (at roughly z = 10 mm). The present measurements generally were within the fuel-rich regions of the flames and ended 5-10 mm after the flame sheet was reached.

Soot (gas) temperatures reach broad maxima at conditions near the maximum soot volume fraction conditions and somewhat before the flame sheet is reached. The maximum measured temperatures are also smaller than the stoichiometric temperatures summarized in Table 1. These trends are qualitatively similar to those of Sunderland et al.[1] and Xu and Faeth[7] for acetylene-fueled and Sunderland and Faeth[2] for hydrocarbon-fueled laminar coflowing jet diffusion flames burning in air.

The results illustrated in Figs. 1-3 show that velocities increase from burner exit values of roughly 0.003 m/s to values in excess of 2 m/s at the highest position that was measured. This is expected due to strong effects of buoyancy as indicated by the relatively

small burner exit Froude numbers and relatively small gas densities compared to ambient gas densities.

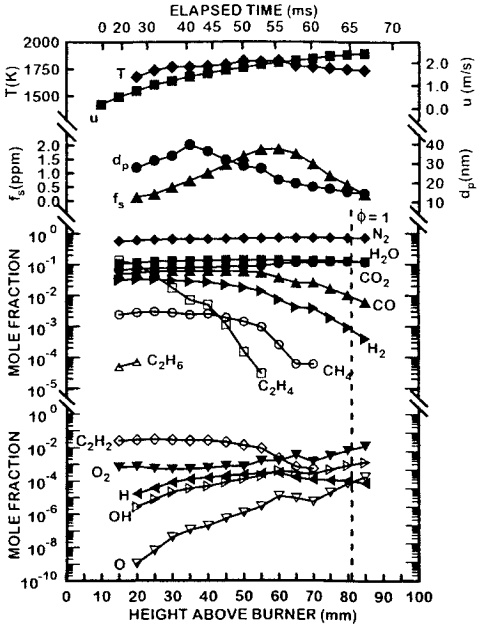

Fig. 1 Measured soot and flame properties along the axis of an ethylene/air laminar jet diffusion flame at roughly atmospheric pressure.

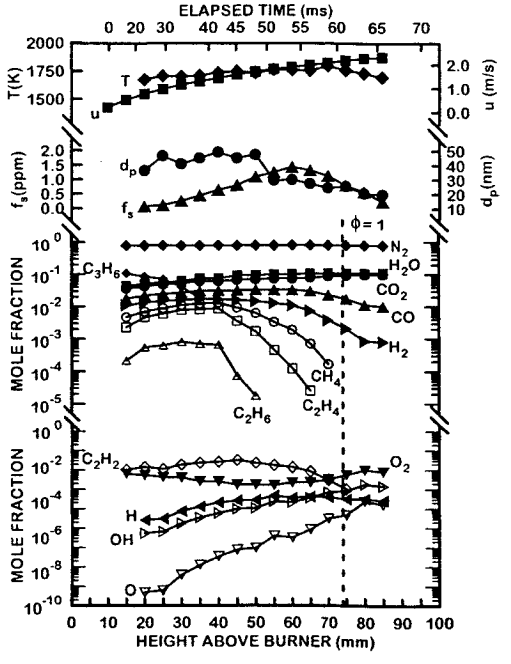

Fig. 2 Measured soot and flame properties along the axis of a propylene-nitrogen/air laminar jet diffusion flame at roughly atmospheric pressure.

Primary soot particle diameters reach maximum values well before the maximum soot volume

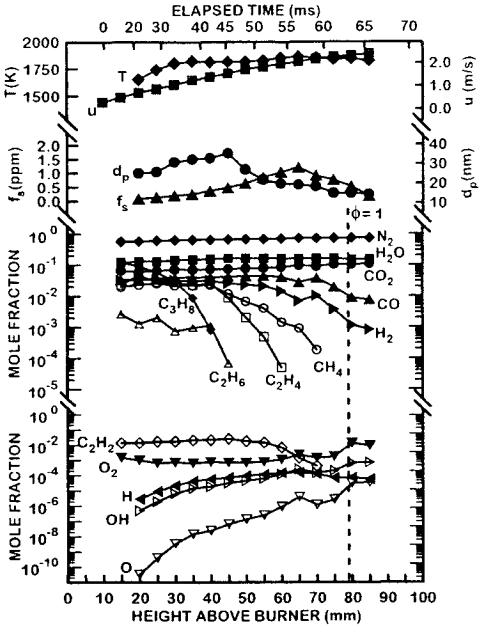

Fig. 3 Measured soot and flame properties along the axis of a propane/air laminar jet diffusion flame at roughly atmospheric pressure.

fraction condition is reached, which is typical of past observations in the soot formation regions of laminar diffusion flames, see Refs. 1-3 and 7. This behavior is caused by accelerating nucleation rates with increasing streamwise distance, as discussed elsewhere,[1-3,7] see Tesner[36,37] for early observations and discussions of this behavior.

The original fuel generally disappears relatively soon within the soot formation region, more robust hydrocarbon species such as ethylene and methane persist to somewhat larger distances from the burner exit, whereas relatively stable acetylene, which is thought to be a major building block of PAH that leads to soot nucleation and to be a major building block of soot growth as well,[9-11,24] appears at relatively large concentrations near to the burner exit and persists at relatively large concentrations (mole fractions greater than 0.001) throughout the region where soot formation dominates soot oxidation (up to the maximum soot volume fraction condition). Acetylene concentrations decrease at a relatively rapid rate, however, within the region where soot oxidation dominates (beyond the maximum soot volume fraction condition). Even though acetylene concentrations are relatively large

near the burner exit, however, significant rates of soot formation are not observed until H, the other major reactant needed to form soot via the HACA mechanism, reaches concentrations greater than 5-10 ppm. Notably, similar concentrations of H were required to obtain significant rates of soot formation in acetylene-fueled diffusion flames.[7] The soot formation region, however, contains significant concentrations of species potentially responsible for soot oxidation, e.g., O_2, C O_2, H_2O, O and OH.[33,34,38-43] Thus, soot formation and soot oxidation proceed at the same time with soot formation dominating the process up to the maximum soot volume fraction position and soot oxidation dominating the process thereafter.

The concentrations of major gas species in Figs. 1-3 are in qualitative agreement with earlier measurements in hydrocarbon-fueled diffusion flames, see Ref. 2. The concentrations of the lower hydrocarbons (CH_4, C_2H_2, C_2H_4) decrease and the concentration of O_2 increases monotonically throughout the soot formation region, whereas, other intermediate hydrocarbons (e.g., C_2H_6) reach maxima before the soot concentration maxima are reached. The combustion products, CO_2 and H_2O, increase slowly throughout the soot formation region, finally reaching broad maxima near the flame sheet (ϕ=1). The intermediate combustion products associated with water-gas equilibrium, H_2 and CO, are both present in large concentrations throughout the soot formation region and reach broad maxima somewhat upstream of the flame sheet. Finally, nitrogen dominates the composition of the ambient air, and of nitrogen-containing fuel streams; therefore, the concentrations of nitrogen are relatively uniform throughout the soot formation regions of the present flames.

The Li/LiOH atomic absorption technique yields concentrations of H, OH and O.[5,7,33,34] These measurements were compared with equilibrium estimates of the concentrations of these radicals that were found using the equilibrium data of Chase et al.[44] and the present measurements of temperature and stable major gas species concentrations. These results show that H concentrations are comparable to equilibrium concentrations, if not somewhat smaller, near the onset of soot formation but eventually reach concentrations 10-20 times larger than equilibrium concentrations at the farthest downstream positions of the present measurements, near the flame sheet. This behavior is similar to earlier observations in acetylene-fueled diffusion flames.[7] Thus, it appears that H generally is present in superequilibrium concentrations throughout the soot formation regions of diffusion flames, compared to near-equilibrium concentrations throughout the soot formation regions of premixed flames.[4-6] This helps explain the more rapid soot surface growth rates observed in diffusion flames, at comparable acetylene concentrations and temperatures, through the HACA mechanism.

Soot Formation Rate Properties

Present measurements were used to study soot surface growth similar to earlier studies using laminar premixed and diffusion flames.[1-7] Major assumptions were identical to the earlier work, as follows: soot surface growth, rather than soot nucleation, dominates soot mass production; effects of diffusion (Brownian motion) and thermophoresis on soot motion are small, so that soot particles convect along the axes of the flames at the local gas velocity; the soot density is constant; and the surface area available for soot surface growth is equivalent to constant diameter spherical primary soot particles that meet at a point. See Refs. 1-7 for justification of these assumptions.

The first soot formation property of importance is the number of primary particles per unit volume, found as follows: [1]

$$n_p = 6f_S/(p\, d_p^3) \qquad (1)$$

The experimental uncertainties (95% confidence) of n_p are estimated to be less than 32% for f_S 0.1 ppm, increasing inversely proportional to f_S for smaller values of f_S. The soot surface area per unit volume is given by: [1]

$$S = 6f_S/d_p \qquad (2)$$

The experimental uncertainties (95% confidence) of S are estimated to be less than 16% for f_S 0.1 ppm, increasing inversely proportional to f_S for smaller values of f_S. Defining the soot surface growth rate as the rate of increase of soot mass per unit surface area and time, conservation of soot mass along a streamline under the previous assumptions gives the soot growth rate as follows:[1]

$$w_g = (\rho/S)\, d(\rho_S f_S/\rho)/dt \qquad (3)$$

where present measurements of species concentrations and temperatures yield the gas density, assuming an ideal gas mixture. The temporal derivative in Eq. 3 was found from three-point least-squares fits of the

argument of the derivative, similar to past work.[1-7] Finally, the soot nucleation rate was defined as the rate of increase of the number of primary particles per unit volume and time; based on previous assumptions, the expression for soot nucleation rates along a streamline becomes: [1]

$$w_n = \rho\, d(n_p/\rho)/dt \qquad (4)$$

Similar to Eq. 3, the temporal derivative in Eq. 4 was found from three-point least-square fits of the argument of the derivative, similar to past work.[1-7]

The four derived soot formation properties (S, n_p, w_g and w_n) are plotted as functions of height along the burner for the three test flames in Fig. 4.

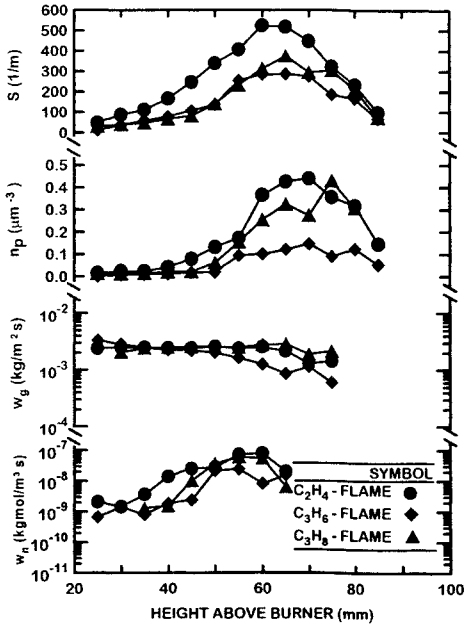

Fig. 4 Derived soot formation properties (S, n_p, w_g and w_n) along the axis of the present hydrocarbon-fueled/air laminar jet diffusion flames at roughly atmospheric pressure.

The soot surface area per unit volume tends to vary similar to soot volume fraction, increasing within the soot formation region and decreasing once again in the soot oxidation region. Values of the number of primary particles per unit volume increase significantly in the region where the primary soot particle diameter reaches a maximum (at z = 40-45 mm) to conditions where the soot volume fraction reaches a maximum (at z = 55-57 mm); it is this behavior that causes primary soot particle diameters to decrease in spite of increased soot concentrations, as discussed earlier. Soot growth rates are relatively constant over the soot growth region, through the HACA mechanism, this behavior follows because progressively increasing values of H are balanced by progressively decreasing values of acetylene. Finally, soot nucleation rates tend to reach a maximum near the maximum soot volume fraction condition, involving somewhat different behavior from soot growth rates, because unlike w_g, w_n does not involve the soot surface area per unit volume, S. The relative values of w_g and w_n should not be generalized to other flame conditions, however, because these rates were simply adjusted to achieve modest soot concentrations in the flames by varying the degree of nitrogen dilution, in order to control problems of measuring soot and flame properties in the present soot-containing flames.

Soot Surface Growth

In order to interpret the present soot surface growth rates, the gross soot surface growth rates from Eq. 3 were corrected for effects of soot oxidation similar to past studies of soot growth in this laboratory.[1-5,7] Thus, estimates of soot growth were limited to conditions where estimated soot oxidation rates never exceeded half the gross soot surface growth rates. This provides a consistent and conservative approach to evaluate effects of soot oxidation that mainly constrains the region where soot growth measurements are obtained with little effect on the values of w_g reported here, see Ref. 7 for a discussion of this issue. Thus, soot oxidation rates were estimated, as follows:[1-5,7] soot oxidation by O and OH was ignored; soot oxidation by O_2 was based on the results of Nagle and Strickland-Constable,[38] which have been confirmed by Park and Appleton;[39] and soot oxidation by H_2O and CO_2 was estimated following Libby and Blake,[40,41] and Johnstone et al.,[42] which gave results similar to Bradley et al.[43]

Soot surface growth rates were interpreted using the HACA soot growth mechanisms of Frenklach and coworkers,[8-10] and Colket and Hall[11] in order to maintain consistency with past evaluations of these mechanisms based on similar measurements and due to the success of these approaches for correlating measurements of soot surface growth in premixed methane/air and methane/oxygen flames[4,5] and in acetylene/air diffusion flames.[7] The predicted net rate of soot surface growth was expressed, as follows, for both mechanisms:

$$w_g = \alpha_i R_i \qquad (5)$$

where i = FW or CH denotes appropriate reaction parameters for the mechanisms of Frenklach and coworkers,[8-10] and Colket and Hall.[11] The parameters, α_i are empirical steric factors of order of magnitude unity, with α_{FW} specified to be a function of temperature,[8-10] and α_{CH} specified to be a constant.[11]

The R_i are proportional to the product $[H][C_2H_2]$ as a first approximation for the earlier premixed flames of Xu et al.,[4,5] the earlier acetylene-fueled diffusion flames of Xu and Faeth[7] and the present hydrocarbon-fueled diffusion flames. Thus, $w_g/[C_2H_2]$ measured for all these studies are plotted as a function of [H] in Fig. 5 in order to provide a direct test of the main features of the HACA soot growth mechanisms without the intrusion of uncertainties due to the numerous empirical parameters of the detailed HACA mechanisms of Refs. 8-11.

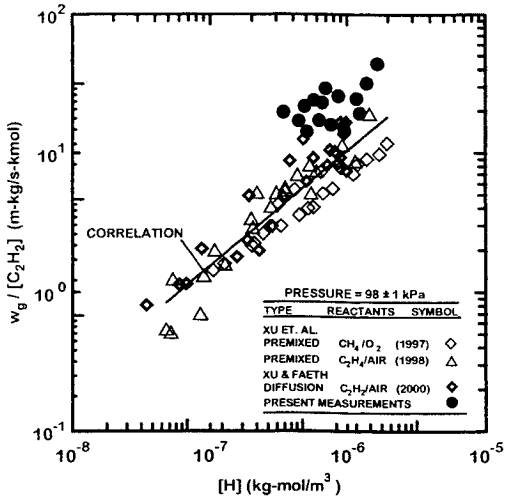

Fig. 5 Soot surface growth rates (corrected for soot oxidation) as a function of acetylene and hydrogen-atom concentrations for laminar premixed and diffusion flames at roughly atmospheric pressure. Measurements of ethylene/air premixed flames from Xu et al.,[4] measurements of methane/oxygen premixed flames from Xu et al.,[5] measurements of acetylene-fueled/air diffusion flames from Xu and Faeth[7] and measurements of hydrocarbon-fueled/air diffusion flames from the present investigation.

The results for premixed and diffusion flames are distinguished in the figures by denoting them by open and closed symbols, respectively. The correlation of previous results for premixed flames and acetylene-fueled diffusion flames is quite good, which is not surprising because acetylene is the dominant hydrocarbon fuel present in both cases. The correlation of the present results for hydrocarbon fuels also is reasonably good but these results indicate systematically larger values of $w_g/[C_2H_2]$ for given values of [H]. This behavior could imply a parallel channel for soot surface growth, other than the HACA mechanism, in the soot formation of diffusion flames for the present hydrocarbon fuels that is not observed for acetylene. In particular, Sunderland et al.[1,2] studied soot growth in both acetylene-fueled and other hydrocarbon-fueled diffusion flames and found similar seemingly enhanced rates of soot growth in the hydrocarbon-fueled flames compared to the acetylene-fueled flames. This possibility will be explored more thoroughly by directly evaluating the HACA mechanism of Refs. 8-11 as discussed in the following.

The direct evaluation of the HACA mechanism of Frenklach and coworkers[8-10] was carried out by plotting w_g directly as a function of $\alpha_{FW} R_{FW}$ as indicated by Eq. 5 in Fig. 6.

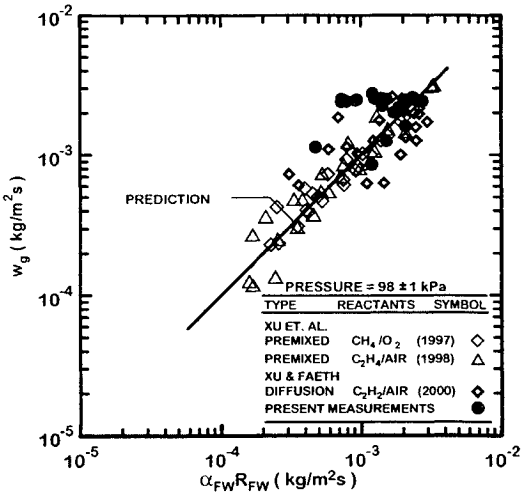

Fig. 6 Soot surface growth rates (corrected for soot oxidation) in terms of the HACA mechanism of Frenklach and coworkers[8-10] for premixed and diffusion flames at roughly atmospheric pressure. Measurements of ethylene/air premixed flames from Xu et al.,[4] measurements of methane/oxygen premixed flames from Xu et al.,[5] measurements of acetylene-fueled/air diffusion flames from Xu and Faeth[7] and measurements of hydrocarbon-fueled/air diffusion flames from the present investigation.

Results for the premixed flames of Xu et al.,[3,4] from acetylene-fueled diffusion flames from Xu and Faeth[7] and from the present hydrocarbon-fueled diffusion flames are illustrated in Fig. 6. The plot represents a direct evaluation of earlier results for premixed flames using $\alpha_{FW}(T)$ from Eq. 6, e.g.,

$$\alpha_{FW}(T) = 0.00154 \exp(12400/T) \quad (6)$$

with T(K). The present results for hydrocarbon-fueled diffusion flames exhibit a slight tendency for enhanced soot growth rates for given values of $[C_2H_2]$, [H] and temperature but the present results for hydrocarbon-fueled diffusion flames generally fall within the experimental uncertainties of the present and earlier measurements. Another evaluation of the HACA soot growth mechanism of Frenklach and coworkers[8-10] is illustrated in Fig. 7, where the correlation of $\alpha_{FW}(T)$ is illustrated for available measurements in both premixed and diffusion flames.

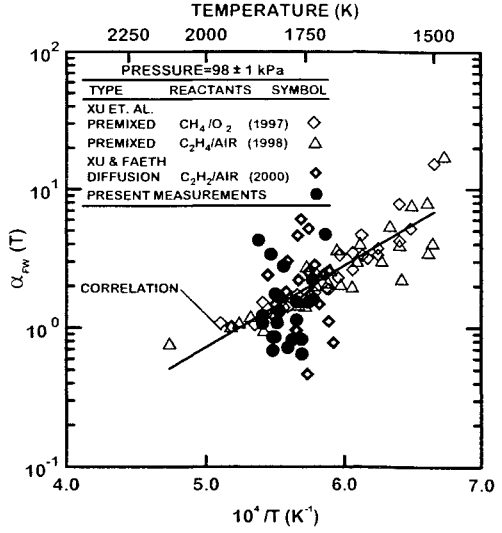

Fig. 7 Correlation of the steric factor for soot growth for the HACA mechanism of Frenklach and coworkers[8-10] as a function of local temperature for premixed and diffusion flames at roughly atmospheric pressure. Measurements of ethylene/air premixed flames from Xu et al.,[4] measurements of methane/oxygen premixed flames from Xu et al.,[5] measurements of acetylene-fueled/air diffusion flames from Xu and Faeth[7] and measurements of hydrocarbon-fueled/air diffusion flames from the present investigation.

The correlation of $\alpha_{FW}(T)$ according to Eq. 6 is also plotted on the figure for reference purposes. Once again, the scatter of the new measurements for the present hydrocarbon-fueled diffusion flames generally falls within the experimental uncertainties of the present and earlier measurements. Taken together, the results of Figs. 6 and 7 provide little motivation to either modify the correlation of Eq. 6 or to suggest the presence of a significant parallel soot growth channel to the HACA measurements of Frenklach and coworkers[8-11] for the premixed and diffusion flames that have been studied thus far.

The corresponding evaluation of the HACA mechanism of soot surface growth due to Colket and Hall[11] is illustrated in Fig. 8. In this case $\alpha = 0.9$ with an uncertainty (95%) of 0.2 from Refs. 4, 5 and 7 proved suitable for present measurements and was used for the predictions illustrated in Fig. 8. The overall correlation illustrated in Fig. 8 is seen to be reasonably effective for both premixed and diffusion flames.

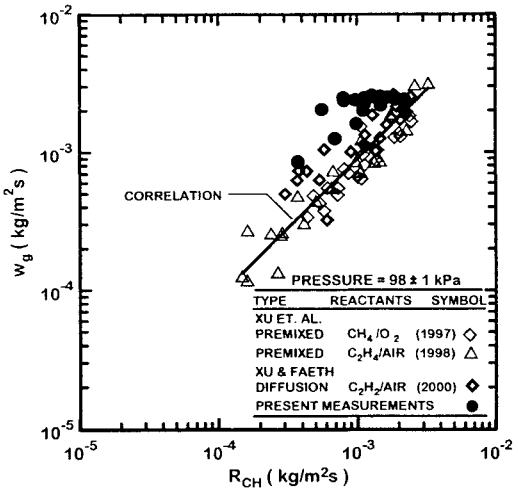

Fig. 8 Soot surface growth rates (corrected for soot oxidation) in terms of the HACA mechanism of Colket and Hall[11] for premixed and diffusion flames at roughly atmospheric pressure. Measurements of ethylene/air premixed flames from Xu et al.,[4] measurements of methane/oxygen premixed flames from Xu et al.,[5] measurements of acetylene-fueled/air diffusion flames from Xu and Faeth[7] and measurements of hydrocarbon-fueled/air diffusion flames from the present investigation.

The present evaluations of the HACA soot surface growth mechanism of Frenklach and coworkers[8-10] and Colket and Hall[11] continue to be very encouraging and these approaches may eventually provide the basis of robust methods to estimate soot surface growth rates in flame environments. Uncertainties remain, however, about the behavior of soot surface growth in diffusion flames fueled by hydrocarbons other than acetylene and the hydrocarbons considered during the present investigation (particularly unsaturated hydrocarbons such as aromatics that could favor the formation of soot by pathways other than the HACA soot surface growth mechanism considered here, e.g., PAH pathways such as those discussed by Howard[24] and about effects of

pressure on soot growth. Finally, processes of soot oxidation are somewhat more important in diffusion flames than in soot-containing premixed flames, and thus effects of soot oxidation on the details of the HACA and PAH soot growth mechanisms must also be quantified.

Conclusions

Flame structure and soot formation processes were studied in coflowing laminar jet diffusion flames. Test conditions involved ethylene-, propylene-, and propane-fueled flames burning in air at atmospheric pressure as summarized in Table 1. The major conclusions of the study are as follows:

1) Measurements show that H, OH and O approach equilibrium near the start of the soot formation region but generally exhibit superequilibrium concentrations (by factors of 10-20 for H and OH and by factors of 10-100 for O) throughout the region; this behavior is quite similar to earlier observations of laminar acetylene-fueled coflowing jet diffusion flames at atmospheric pressure.

2) Measurements show that significant degrees of net soot formation only occurs in regions where reasonable concentrations of both H and acetylene are present; this behavior is similar to earlier observations of laminar acetylene-fueled coflowing jet diffusion flames at atmospheric pressure.[7]

3) Soot surface growth rates in the present hydrocarbon-fueled laminar jet diffusion flames were in good agreement with past measurements in both laminar premixed flames[4,5] and acetylene-fueled laminar jet diffusion flames and could be correlated by the HACA soot growth mechanisms of Frenklach and coworkers[8-10] and Colket and Hall,[11] with steric factors in each of these theories correlating in the same manner for all flame conditions that have been studied.

Acknowledgments

This research was supported by NASA Grants NCC3-661, NAG3-1878, NAG3-2038 and NAG3-2404 under the technical management of D. L. Urban and Z.-G. Yuan of the NASA Glenn Research Center.

References

[1]Sunderland, P.B., Köylü, Ü.Ö., and Faeth, G.M., "Soot Formation in Weakly Buoyant Acetylene-Fueled Laminar Jet Diffusion Flames Burning in Air," *Combustion and Flame*, Vol. 100, Nos. 1/2, 1995, pp. 310-322.

[2]Sunderland, P.B., and Faeth, G.M., "Soot Formation in Hydrocarbon/Air Laminar Jet Diffusion Flames," *Combustion and Flame*, Vol. 105, Nos. 1/2, 1996, pp. 132-146.

[3]Lin, K.-C., Sunderland, P.B., and Faeth, G.M., "Soot Nucleation and Growth in Acetylene/Air Laminar Coflowing Jet Diffusion Flames," *Combustion and Flame*, Vol. 104, No. 3, 1996, pp. 369-375.

[4]Xu, F., Sunderland, P.B., and Faeth, G.M., "Soot Formation in Laminar Premixed Ethylene/Air Flames at Atmospheric Pressure," *Combustion and Flame*, Vol. 108, No. 4, 1997, pp. 471-493.

[5]Xu, F., Lin, K.-C., and Faeth, G.M., "Soot Formation in Laminar Premixed Methane/Oxygen Flames at Atmospheric Pressure," *Combustion and Flame*, Vol. 115, Nos. 1/2, 1998, pp. 195-209.

[6]Xu, F., and Faeth, G.M., "Structure of the Soot Growth Region of Laminar Premixed Methane/Oxygen Flames," *Combustion and Flame*, Vol. 121, No. 4, 2000, pp. 640-650.

[7]Xu, F., and Faeth, G.M., "Soot Formation in Laminar Acetylene/Air Diffusion Flames at Atmospheric Pressure," *Combustion and Flame*, in press.

[8]Frenklach, M., and Wang, H. "Detailed Modeling of Soot Particle Nucleation and Growth," *Proceedings of the Combustion Institute,* Vol. 23, 1990, pp. 1559-1556.

[9]Frenklach, M., and Wang, H., "Detailed Mechanism and Modeling of Soot Particle Formation," *Soot Formation in Combustion* (H. Bockhorn, ed.), Springer-Verlag, Berlin, 1994, p. 165-192.

[10]Kazakov, A.,Wang, H., and Frenklach, M., "Detailed Modeling of Soot Formation in Laminar Premixed Ethylene Flames at a Pressure of 10 Bar," *Combustion and Flame*, Vol. 100, Nos. 1/2, 1995, pp. 111-120.

[11]Colket, M.B., and Hall, R.J., "Successes and Uncertainties in Modeling Soot Formation in Laminar

Premixed Flames," *Soot Formation in Combustion* (H. Bockhorn, ed.), Springer-Verlag, Berlin, 1994, p. 442-470.

[12]Balthasar, M., Heyl, A., Mauss, F., Schmitt, F., and Bockhorn, H., "Flamelet Modeling of Soot Formation in Laminar EthyleneAir-Diffusion Flames," *Proceedings of the Combustion Institute,* Vol. 26, 1996, pp. 2369-2377.

[13]Bai, K.W., Balthasar, M., Mauss, F., and Fuchs, L., "Detailed Soot Modeling in Turbulent Jet Diffusion Flames," *Proceedings of the Combustion Institute,* Vol. 27, 1998, pp. 1623-1630.

[14]Mitchell, R.E., Sarofim, A.F., and Clomberg, L.A., "Experimental and Numerical Investigation of Confined Laminar Diffusion Flames," *Combustion and Flame*, Vol. 37, No. 3, 1980, pp. 227-244.

[15]Santoro, R.J., Semerjian, H.B., and Dobbins, R.A., "Soot Particle Measurements in Diffusion Flames," *Combustion and Flame*, Vol. 51, No. 2, 1983, pp. 203-218.

[16]Smyth, K.C., Miller, J.H., Dorfman, R.C., Mallard, W.G., and Santoro, R.J., "Soot Inception in a Methane/Air Diffusion Flame as Characterized by Detailed Species Profiles," *Combustion and Flame*, Vol. 62, No. 2, 1985, pp. 157-181.

[17]Santoro, R.J., Yeh, T.T., Horvath, J.J., and Semerjian, H.G., "The Transport and Growth of Soot Particles in Laminar Diffusion Flames," *Combustion Science and Technology,* Vol. 53, Nos. 2+3, 1987, pp. 89-115.

[18]Puri, R., Santoro, R.J., and Smyth, K.C., "The Oxidation of Soot and Carbon Monoxide in Hydrocarbon Diffusion Flames," *Combustion and Flame*, Vol. 97, No. 2, 1994, pp. 125-144.

[19]Puri, R., Santoro, R.J., and Smyth, K.C., "The Oxidation of Soot and Carbon Monoxide in Hydrocarbon Diffusion Flames," *Combustion and Flame*, Vol. 102, Nos. 1/2, 1995, pp. 226-228.

[20]Saito, K., Williams, F.A., and Gordon, A.S., "Structure of Laminar Coflow Methane-Air Diffusion Flames," *Journal of Heat Transfer,* Vol. 108, No. 3, 1986, pp. 640-648.

[21]Garo, A., Lahaye, J., and Prado, G., "Mechanisms of Formation and Destruction of Soot Particles in a Laminar Methane-Air Diffusion Flame," *Proceedings of the Combustion Institute,* Vol. 21, 1986, pp. 1023-1031.

[22]Garo, A., Prado, G., and Lahaye, J., "Chemical Aspects of Soot Particles Oxidation in a Laminar Methane-Air Diffusion Flame," *Combustion and Flame*, Vol. 79, Nos. 3 and 4, 1990, pp. 226-233.

[23]Haynes, B. S., and Wagner, H. G., "Soot Formation," *Progress in Energy and Combustion Science*, Vol. 7, No. 4, 1981, pp. 229-273.

[24]Howard, J.B., "Carbon Addition and Oxidation Reactions in Heterogeneous Combustion and Soot Formation," *Proceedings of the Combustion Institute,* Vol. 23, 1990, pp. 1107-1127.

[25]Glassman, I., "Soot Formation in Combustion Processes," *Proceedings of the Combustion Institute*, Vol. 22, 1988, pp. 295-311.

[26]Hardiquert, M., Cessou, A., Stepowski, D., and Coppalle, A., "OH and Soot Concentration Measurements in a High-Temperature Laminar Diffusion Flame," *Combustion and Flame,* Vol. 111, No. 4, 1997, pp. pp. 338-349.

[27]McEnally, C.S., and Pfefferle, L.D., "Aromatic and Linear Hydrocarbon Concentration Measurements in a Non-Premixed Flame," *Combustion Science and Technology,* Vols. 115-117, Nos. 1-6, 1996, pp. 183-209.

[28]McEnally, C.S., and Pfefferle, L.D., "Flow Time Effects on Hydrocarbon Growth and Soot Formation in Coflowing Methane/Air Non-Premixed Flames," *Proceedings of the Combustion Institute,* Vol. 27, 1998, pp. 1539-1547.

[29]Dalzell, W.H., and Sarofim, A.F., "Optical Constants of Soot and Their Application to Heat Flux Calculations," *Journal of Heat Transfer.* Vol. 91, No. 1, 1969, pp. 100-104.

[30]Krishnan, S.S., Lin, K.-C., and Faeth, G.M., "Optical Properties in the Visible of Overfire Soot in Large Buoyant Turbulent Diffusion Flames," *Journal of Heat Transfer,* Vol. 122, No. 3, 2000, pp. 517-524.

[31]Dobbins, R.A., and Megaridis, C.M. "Morphology of Flame-Generated Soot as Determined by Thermophoretic Sampling," *Langmuir*, Vol. 3, No. 2, 1982, pp. 254-259.

[32]Köylü, Ü.Ö., and Faeth, G.M., "Structure of Overfire Soot in Buoyant Turbulent Diffusion Flames at Long Residence Times," *Combustion and Flame,* Vol. 89, No. 2, 1992, pp. 140-156.

[33]Neoh, K.G., Howard, J.B., and Sarofim, A.F., "Soot Oxidation in Flames," *Particulate Carbon* (D.C. Siegla and B.W. Smith, ed.), Plenum Press, New York, 1980, pp. 261-277.

[34]Neoh, K.G., *Soot Burnout in Flames*, Ph.D. Thesis, Massachusetts Institute of Technology, Cambridge, MA, 1980.

[35]McBride, B.J., Reno, M.A., and Gordon, S., *CET93 and CETPC: An Interim Updated Version of the NASA Lewis Computer Program for Calculating Complex Chemical Equilibrium with Applications*, NASA Technical Memorandum 4557, Washington, D.C., 1994.

[36]Tesner, P.A., "Formation of Dispersed Carbon by Thermal Decomposition of Hydrocarbons," *Proceedings of the Combustion Institute,* Vol. 7, 1958, pp. 546-556.

[37]Tesner, P.A., "Dispersed Carbon Formation by Acetylene Self-Combustion," *Proceedings of the Combustion Institute,* Vol. 8, 1960, pp. 627-633.

[38]Nagle, J., and Strickland-Constable, R.F., "Oxidation of Carbon Between 1000-2000 C," *Proceedings of Fifth Carbon Conference*, Vol. 1, 1962, pp. 154-164.

[39]Park, C., and Appleton, J.P., "Shock-Tube Measurements of Soot Oxidation Rates," *Combustion and Flame,* Vol. 20, No. 3, 1973, pp. 369-379.

[40]Libby, P.A., and Blake, T.R., "Theoretical Study of Burning of Carbon Particles," *Combustion and Flame*, Vol. 36, No. 2, 1979, pp. 139-169.

[41]Libby, P.A., and Blake, T.R., "Burning of Carbon Particles in the Presence of Water Vapor," *Combustion and Flame,* Vol. 41, No. 2, 1981, pp. 123-147.

[42]Johnstone, J.F., Chen, C.Y., and Scott, D.S., "Kinetics of the Steam-Carbon Reaction in Porous Graphite," *Industrial Engineering Chemistry,* Vol. 44, 1952, pp. 1564-1569.

[43]Bradley, D., Dixon-Lewis, G., El-Din Habik, S., and Mushi, E.M.J., "The Oxidation of Graphite Powder in Flame Reaction Zones," *Proceedings of the Combustion Institute,* Vol. 20, 1984, pp. 931-940.

[44]Chase, M.W., Jr., Davies, C.A., Downey, J.R., Jr., Frurip, D.J., McDonald, R.A., and Syverud, A.N., *JANAF Thermochemical Tables*, 3rd ed., *Journal of Physical Chemistry Reference Data*, Vol. 14, Supplement No. 1, 1986, p. 1211.